Three-dimensional proton trajectory analyses and simulation of neutral particle transport in an ICRF heated long pulse discharge on the large helical device

Three-dimensional simulation of neutral particle transport in ICRF heated long pulse discharges on the large helical device

M. Shoji[a], R. Kumazawa[a], K. Saito[a], T. Watanabe[a], Y. Nakamura[a], S. Masuzaki[a], S. Morita[a], M. Goto[a], N. Noda[a], N.Ohyabu[a] and LHD Experimental Groups[a]

[a]*National Institute for Fusion Science, Toki, 509-5292, Japan*

Abstract

Three-dimensional neutral particle transport simulation code is used to identify a source of the hydrogen outgas in a LHD long pulse discharge by ICRF heating. Radiation collapse induced by uncontrollable plasma density rise terminated the long pulse discharges. Torodially non-uniform increases in the H_α emission and divertor temperature were observed. A CCD camera detected local heating of a vertically installed divertor plate, which is consistent with the strike points of the trajectories of protons accelerated by ICRF waves. The neutral particle transport simulation with the trajectory analyses of the protons shows that outgas from the divertor plates heated by the protons is necessary for explaining the observed toroidal non-uniform distribution of the H_α emission during the long pulse discharge.

PACS: 52.40.Hf

JNM keywords: Carbon, Divertor Materials, Hydrogen and Hydrides, Plasma-Materials Interaction, Theory and Modeling

PSI-16 keywords: DEGAS, ICRF, LHD, Neutrals, Steady State

Presenting author: Mamoru Shoji

Presenting author e-mail: shoji@LHD.nifs.ac.jp

1. Introduction

Plasma wall interactions in long pulse discharges are one of the critical issues in optimizing the first wall materials or the divertor design for future nuclear fusion reactors. The large helical device (LHD) has an advantage in long pulse discharge experiments due to the superconducting magnetic coils and non plasma-current operation [1]. We investigate the neutral particle transport induced by the plasma-wall interactions in LHD long pulse discharges heated by ion cyclotron range of frequency (ICRF) heating. In the next section, experimental setup for the long pulse discharges is depicted, and the experimental results are shown in section 3. Analyses on the proton trajectories and neutral particle transport are described in section 4. In the last section, we propose a possible solution for steady state plasma operation with the conclusion of this paper.

2. Experimental set-up for long pulse discharges

Figure 1 gives a bird's eye view of the cross-section of the LHD vacuum vessel with plasma heating and diagnostic systems for long pulse discharges. The five kinds of vacuum ports (inner, outer, upper, lower and tangential ports) are equipped. Four divertor legs and ergodic layer are formed outside of the main plasma, and divertor plates (carbon) are installed along strike points of the divertor legs on the vacuum vessel. Thermocouples are embedded in some divertor plates for temperature measurement [2].

Three pairs of ICRF antennas with carbon protectors are installed in port-3.5, 4.5 and 7.5. The antennas consist of upper and lower parts supported from the upper and lower ports, respectively. In the long pulse discharges, a minority heating method was employed in majority helium plasmas with hydrogen as the minority ions. The ion cyclotron resonance (ICR) layer was located at the saddle point of the mod-*B* surface for optimizing heating efficiency [3]. The toroidal distribution of neutral hydrogen has been measured with single channel H_α emission detectors mounted on all outer ports. A visible CCD camera mounted on an outer port observed divertor plates and the divertor legs near a lower port.

3. Experimental results in a long pulse discharge by ICRF heating

We succeeded in sustaining plasma for 150 seconds by ICRF heating [4]. The plasma parameters were as follows: the average electron density n_e=5~6x10^{18} m^{-3}, the central electron and ion temperature T_{e0}~T_{i0}~2 keV, and the ICRF heating power P_{ICH}~500 kW. One ICRF antenna installed in port-3.5 was used in this discharge. The plasma was terminated by uncontrollable plasma density rise with gradually increase in the H_α intensity in the later phase of the discharge (after t=100 sec.) as shown in Figure 2. The radiation power P_{rad} and impurity emission (CIII, OV) also exhibited similar time evolution. The increment in the H_α intensity is observable compared to that of impurities. Figure 3 illustrates the toroidal distribution of the H_α intensity ratio $I_{H\alpha}^{150s}/I_{H\alpha}^{90s}$, where $I_{H\alpha}^{150s}$ and $I_{H\alpha}^{90s}$ are the intensity measured at t=150 and 90 sec., respectively, showing a peaked profile around port-3, and closed circles represent the temperature of the divertor plates installed near inner ports, which also exhibits a local heating of the divertor plates around port-3. The CCD camera observed

local heating of a vertically installed divertor plate installed near the port-3. These experimental results indicate that local hydrogen outgas was induced by heating of the divertor plates around port-3 during the long pulse discharge.

4. Three-dimensional neutral particle transport simulation

We calculated the trajectories of protons accelerated by ICRF waves excited from the antenna installed in port-3.5. Figure 4 gives the toroidal and poloidal distribution of the calculated strike points with colored squares which express the observed incremental temperature of the divertor plates. In this figure, the toroidal angle ϕ of 0 degree is the position where the plasma is horizontally elongated, and the poloidal angle θ of 0 degree means the outboard side of the torus. The distribution of the strike points is consistent with that of the incremental temperature of divertor plates. We, thus, consider the following three possible sources of strong outgas around port-3:

Case 1: the vertically installed divertor plate locally heated by the accelerated protons,
Case 2: the protectors for the ICRF antenna heated by a RF current and a plasma heat load,
Case 3: the several divertor plates heated by the protons accelerated by the ICRF waves.

Density profile of neutral hydrogen is computed by a neutral particle transport simulation code (DEGAS ver.63) for the above three cases [5]. In the simulation, test particles representing neutral hydrogen are launched into a three-dimensional grid model for the LHD configuration. The plasma parameter profiles in the grid model are determined on the basis of the measurements of plasma diagnostic systems. Test particles (neutral hydrogen molecules) are emitted from the vertically installed divertor plate (case 1) and from the protector (case 2). In case 3, the toroidal distribution of the hydrogen outgas from the divertor plates is determined on the basis of the calculations of the proton trajectory analyses.

The calculated density profile of atomic hydrogen in the above three cases are shown in Figure 5. Hydrogen atoms are locally concentrated near the divertor plate (in case 1) and the protector (in case 2). The complicated shape of the LHD plasma and the vacuum vessel can obstruct toroidal diffusion of the neutral particles. In case 3, the neutral atoms widely spread because of the toroidally distributed sources of the hydrogen outgas. The toroidal distribution of the H_α intensity in the three cases ($\Delta I_{H\alpha}^{\text{by ICRF}}$) is obtained by integrating the calculated H_α emission along the line of sight of the detectors. Figure 6 (a) is the toroidal distribution of the H_α intensity in the three cases, in which the intensity is normalized to that in port-3. Figure 6 (b) shows the toroidal distribution of the observed ratio of the H_α intensity ($I_{H\alpha}^{150}/I_{H\alpha}^{90}$). We regard the average value of the ratio measured in port-6, 7 and 8 as a background ratio caused by usual plasma-wall interactions without the effect of the accelerated protons. Comparison between the calculations and the observation (the background ratio should be subtracted) shows that the H_α intensity in case 1 and 2 is strongly peaked around port-3, which is not consistent with the observation. The toroidally distributed sources of hydrogen outgas in case 3 can explain the observed toroidal distribution of H_α intensity rise in the long pulse discharge.

5. Conclusion

Uncontrollable plasma density rise occurred in the later phase of a LHD long pulse discharge by ICRF heating. Toroidaly non-uniform increase of the divertor plate temperature and the H_α emission intensity were observed. The distribution of the temperature increase of the divertor plates is consistent with that of the strike points of accelerated protons by the ICRF waves. Neutral particle transport simulation shows that the hydrogen outgas from the divertor plates heated by the protons can explain the observation of the H_α intensity rise. It strongly suggests that the reduction of outgas from the divertor plates installed at the strike points of the protons is effective for sustaining long pulse discharges in LHD.

Acknowledgements

The authors gratefully acknowledge Professor O. Motojima for his encouragement. The author (M.S.) would like to thank technical officers in department of engineering and technical services in NIFS for their experimental support.

References

[1] O. Motojima et al., Phys. Plasmas 6 (1999) 1843.
[2] S. Masuzaki et al., J. Nucl. Mater., 240-243 (2001) 12.
[3] R. Kumazawa et al., Plasma Phys. Control. Fusion 45 (2003) 1037.
[4] K. Saito et al., these Proceedings.
[5] D.B. Heifetz et al., J. Comput. Phys. 46 (1982) 309.

Figure Captions

Fig. 1. Bird's eye view of the cross-section of the vacuum vessel with plasma heating and diagnostic systems for long pulse discharges by ICRF heating. The lines of sight of the H_α emission detectors mounted on all outer ports are also depicted.

Fig. 2. Time evolution of typical plasma parameters (electron density n_e, radiation power P_{rad}, impurity radiation from CIII and OV and intensity of H_α and HeI) in the long pulse discharge.

Fig. 3. Toroidal distribution of the ratio of the H_α intensity at 90 and 150 sec. (colored columns), and the temperature distribution of divertor plates installed near inner ports (black points).

Fig. 4. The toroidal and poloidal distribution of the strike points of accelerated protons by ICRF waves from the upper (red crosses) and lower antennas (blue open circles), and temperature increments of the divertor plates (colored squares) during ICRF heating. The position of the ICRF antennas and the vertically installed divertor plate are also showed.

Fig. 5. The calculations of the three-dimensional distribution of atomic hydrogen density in the grid model between port-2 and port-3 in the three different cases of the hydrogen outgas.

Fig. 6. Calculations of the toroidal distribution of the normalized H_α intensity in the three different cases of the hydrogen outgas (a), and the measured ratio of the H_α intensity at 90 and 150 sec. in the long pulse discharge (b).

Figures

Figure 1

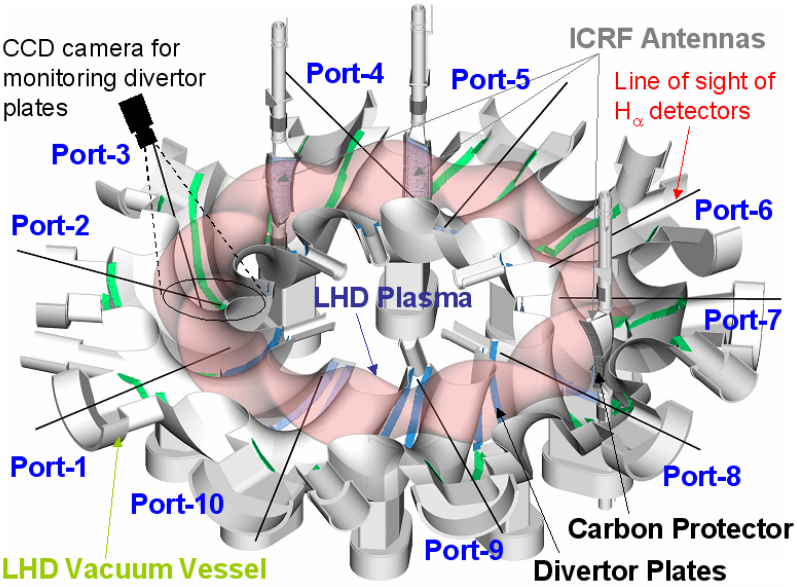

Figure 2

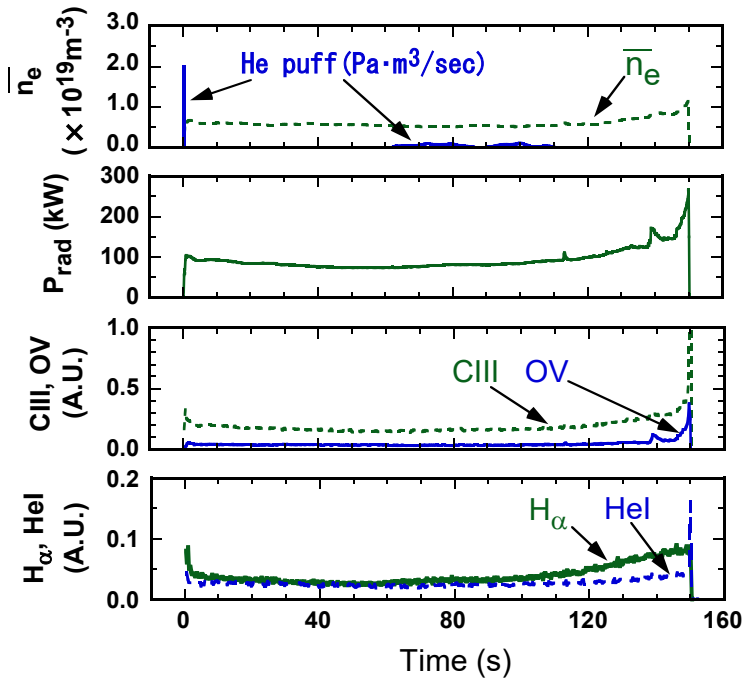
$\bar{n}_e$ ($\times 10^{19}$m^{-3})
3.0
2.0
1.0
0.0
He puff (Pa·m^3/sec)
$\bar{n}_e$
P_{rad} (kW)
300
200
100
0
CIII, OV (A.U.)
1.0
0.5
0.0
CIII
OV
H_α, HeI (A.U.)
0.2
0.1
0.0
H_α
HeI
0
40
80
120
160
Time (s)

Figure 3

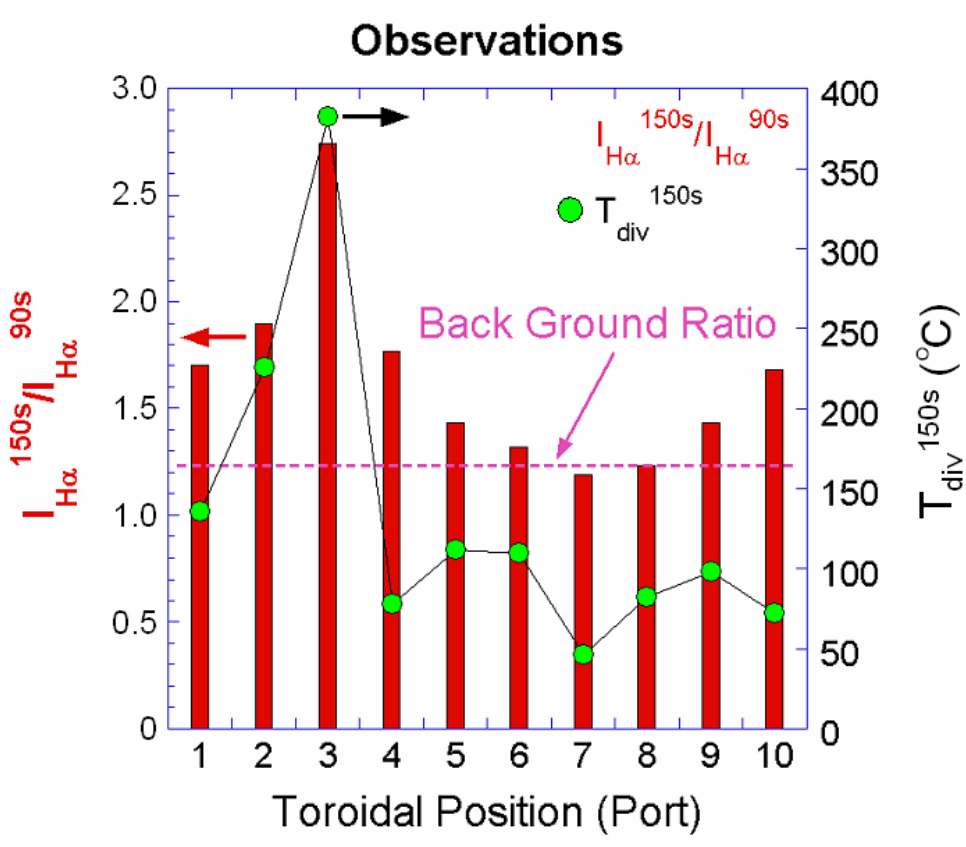
Observations
3.0
2.5
2.0
1.5
1.0
0.5
0
400
350
300
250
200
150
100
50
0
1
2
3
4
5
6
7
8
9
10
Toroidal Position (Port)
I Hα 150s/I Hα 90s
T div 150s
Back Ground Ratio
I Hα 150s/I Hα 90s
T div 150s (°C)

Figure 4

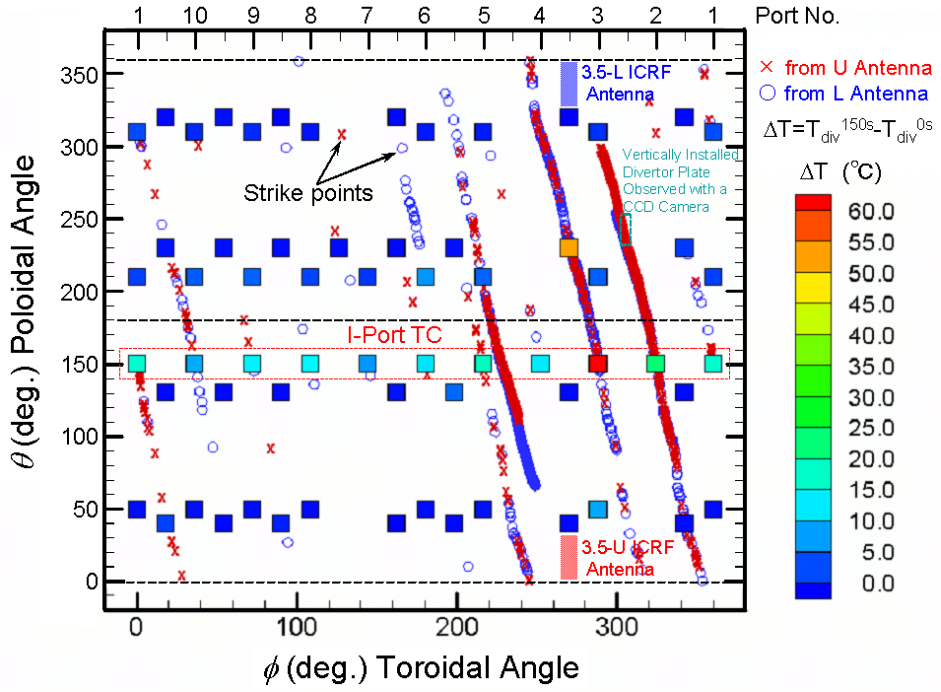
Port No.
1 10 9 8 7 6 5 4 3 2 1
θ (deg.) Poloidal Angle
φ (deg.) Toroidal Angle
0 50 100 150 200 250 300 350
0 100 200 300
3.5-L ICRF Antenna
3.5-U ICRF Antenna
Strike points
I-Port TC
Vertically Installed Divertor Plate Observed with a CCD Camera
× from U Antenna
○ from L Antenna
ΔT=T_div^150s-T_div^0s
ΔT (℃)
60.0
55.0
50.0
45.0
40.0
35.0
30.0
25.0
20.0
15.0
10.0
5.0
0.0

Figure 5

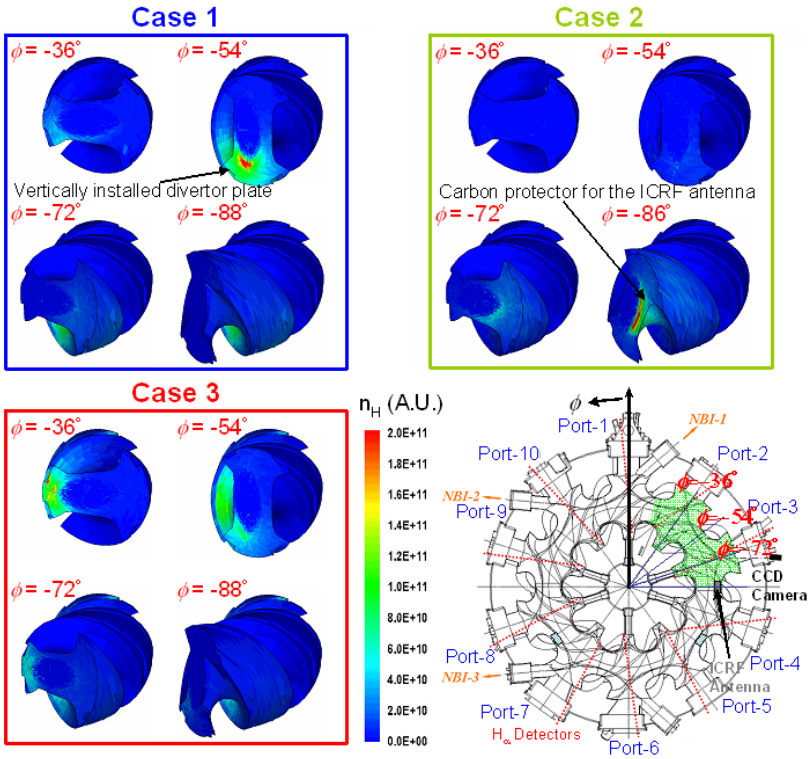
Case 1
ϕ = -36°
ϕ = -54°
Vertically installed divertor plate
ϕ = -72°
ϕ = -88°
Case 2
ϕ = -36°
ϕ = -54°
Carbon protector for the ICRF antenna
ϕ = -72°
ϕ = -86°
Case 3
ϕ = -36°
ϕ = -54°
ϕ = -72°
ϕ = -88°
n_H (A.U.)
2.0E+11
1.8E+11
1.6E+11
1.4E+11
1.2E+11
1.0E+11
8.0E+10
6.0E+10
4.0E+10
2.0E+10
0.0E+00
ϕ
Port-1
NBI-1
Port-10
Port-2
NBI-2
Port-9
Port-3
-36
-54
-72
CCD Camera
Port-8
NBI-3
ICRF Antenna
Port-4
Port-7
Hα Detectors
Port-5
Port-6

Figure 6

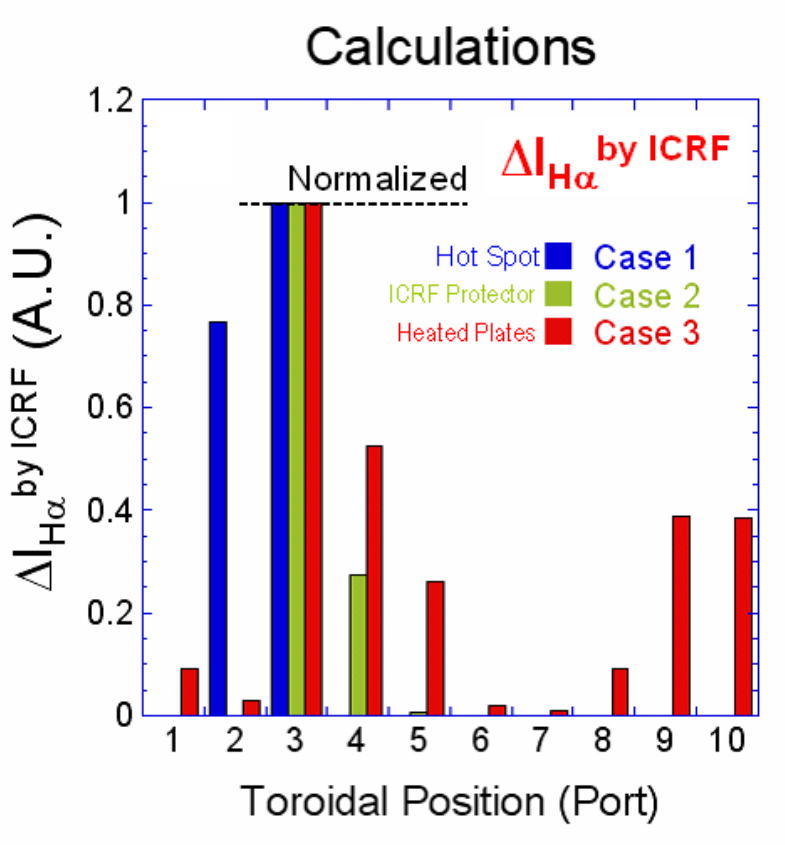
Calculations
$\Delta I_{H\alpha}$ by ICRF
Normalized
Hot Spot Case 1
ICRF Protector Case 2
Heated Plates Case 3
$\Delta I_{H\alpha}$ by ICRF (A.U.)
Toroidal Position (Port)
0
0.2
0.4
0.6
0.8
1
1.2
1
2
3
4
5
6
7
8
9
10